

## Wideband Single-Feed Circularly Polarized Antenna

Weilong Liang\*, Yong-Chang Jiao, Li Zhang, and Tao Ni

**Abstract**—In this paper, a novel wideband single-feed circularly polarized patch antenna is presented. The antenna consists of an L-shaped probe, four parasitic patches perpendicular to the probe, and a planar reflector. By modifying the structure of the patches, two orthogonal radiation modes are created to realize the circular polarization in the broadside direction. This antenna exhibits a wide impedance bandwidth of 82.4% from 2 GHz to 4.8 GHz for the voltage standing wave ratio (VSWR)  $\leq 2$  and a 3-dB axial ratio (AR) bandwidth of 56.2% from 2.11 GHz to 3.77 GHz, over which the antenna gains vary from 5.7 dBic to 9.7 dBic. The measured results agree well with the simulated ones.

### 1. INTRODUCTION

Circularly polarized antennas are of great importance in modern wireless communication, radar, RFID and sensor systems, due to their stability of signal reception and smashing mobility. Recently, patch antennas have attracted increasing attention as an approach for realizing the circular polarization [1–7]. By using four sequential-rotation proximity-coupled L-probes, the antenna in [1] delivers a measured 3-dB axial ratio bandwidth of 82% from 1 to 2.4 GHz. Four sequentially-rotated-fed linearly polarized disks located in a cavity-backed circular slot are used in [2], and the 3-dB axial ratio bandwidth of this antenna is 54.5%. But the feeding network in [1, 2] needs large space and increase complexity of the antenna design. Therefore, the single-feed circularly polarized patch antenna has received much attention for its simple structure. In [3], the circularly polarized antenna has a lower notched circular patch with a capacitive feeding and an upper parasitic notched patch, and its 3-dB axial ratio bandwidth is 10%. By using the horizontally meandered strip (HMS) feed technique, the circular polarization bandwidth can be enhanced to 13.5% [4]. An H-shaped patch antenna is presented in [5]. This antenna features a much wider axial ratio bandwidth of 19.4%. In [6], a novel cross-dipole and curved-delay feeding line are proposed. The antenna has a 3-dB axial ratio bandwidth of 27%. It can be seen that the axial ratio bandwidth of the single-feed circularly polarized antenna is usually very narrow, though its structure is simple.

In this paper, in order to enhance the bandwidth of the single-feed circularly polarized antenna, a novel patch antenna with parasitic elements is presented. This antenna is composed of an L-shaped probe and four parasitic patches located perpendicularly to the probe. By slicing pairs of rectangular and L-shaped slots on the patches, wide impedance bandwidth and 3-dB axial ratio bandwidth can be achieved. Experimentally, the proposed antenna delivers an impedance bandwidth of 82.4% and a 3-dB axial ratio bandwidth of 56.2%. Compared with the single-feed patch antennas in [3–7], this antenna has a much wider axial ratio bandwidth of 56.2%.

---

*Received 20 May 2015, Accepted 9 July 2015, Scheduled 24 July 2015*

\* Corresponding author: Weilong Liang (lw1989@163.com).

The authors are with the National Key Laboratory of Antennas and Microwave Technology, Xidian University, Xi'an, Shaanxi, P. R. China.

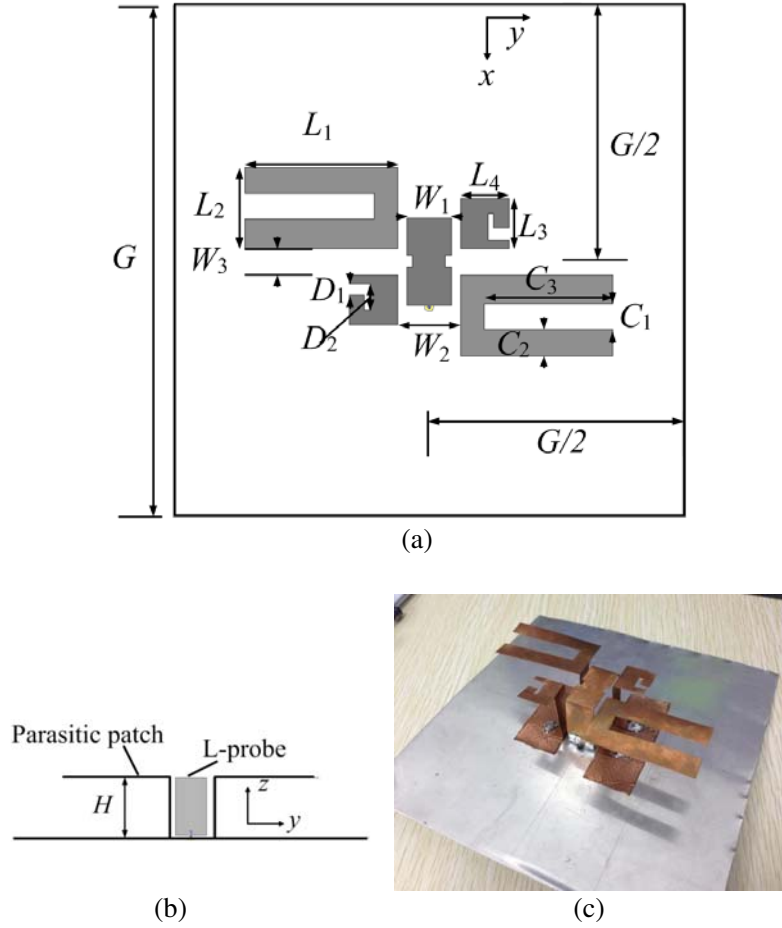


**Figure 1.** Structure and photograph of the proposed antenna. (a) Top view. (b) Front view. (c) Photograph.

## 2. CONFIGURATION AND DESIGN

Figure 1 shows the structure and photograph of the proposed antenna. This antenna consists of an L-shaped probe connecting to an SMA connector and four parasitic radiation elements perpendicular to the probe. The height of the probe is the same as the parasitic elements. The thickness of the metallic structure is 0.1 mm. The parasitic patches are connected to the ground plane. Furthermore, one pair of parasitic patches has smaller dimensions while another pair has large dimensions in order to broaden the impedance bandwidth. By the capacitive coupling, part of the energy is conveyed from the probe to the parasitic patches, which generates a new radiation mode orthogonal to the probe for the circular polarization. To improve the 3-dB axial ratio bandwidth of this antenna, rectangular slots and L-shaped slots are etched on the parasitic patches, respectively, which increase the surface current on the parasitic patches. Detailed dimensions of the antenna are summarized in Table 1.

**Table 1.** Detailed dimensions of the proposed antenna.

Parameter	$C_1$	$C_2$	$C_3$	$D_1$	$D_2$	$G$	$H$
Value (mm)	9	9.8	42	4	8	170	28.5
Parameter	$L_1$	$L_2$	$L_3$	$L_4$	$W_1$	$W_2$	$W_3$
Value (mm)	50.6	27	16.6	16	14.9	18.9	8.7

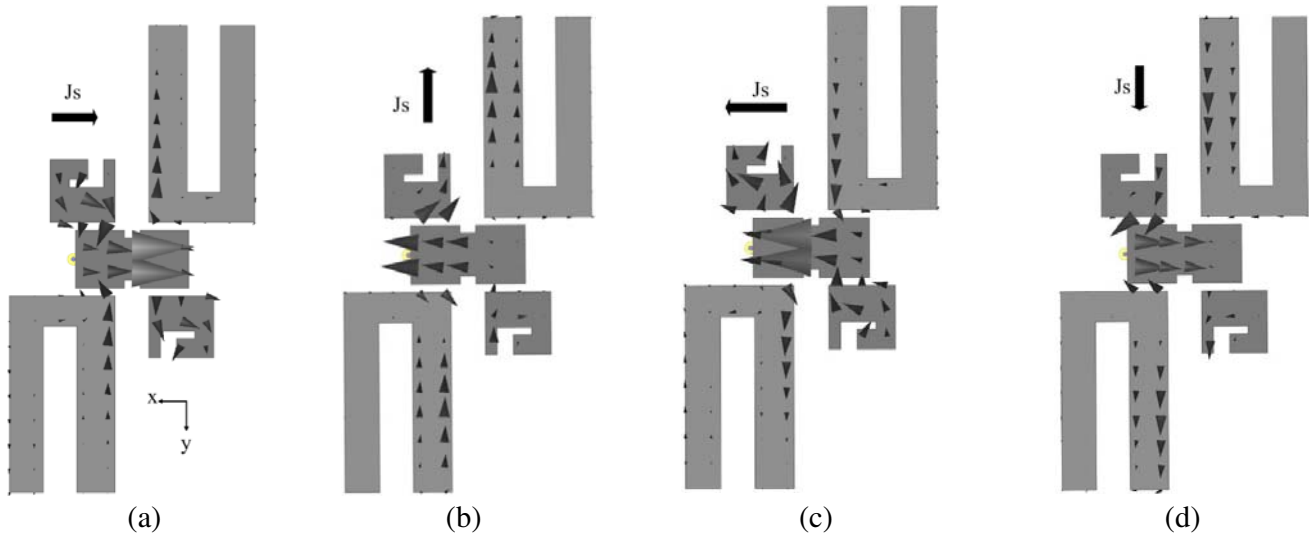


**Figure 2.** Simulated surface current distributions of the proposed antenna at 2.9 GHz. (a)  $\omega t = 0^\circ$ , (b)  $\omega t = 90^\circ$ , (c)  $\omega t = 180^\circ$ , (d)  $\omega t = 270^\circ$ .

In order to explain the circular polarization mode clearly, the surface currents on the patches are analyzed. Fig. 2 shows the simulated surface currents for four different time phases ( $\omega t$ ), from  $0^\circ$  to  $270^\circ$ , with an interval of  $90^\circ$ , at 2.9 GHz. At  $\omega t = 0^\circ$ , the surface current on the probe flows in  $-x$  direction, while the surface currents on the longer and shorter parasitic patches are in the opposite direction. So the predominant surface current is in  $-x$  direction. Also when  $\omega t = 180^\circ$ , the currents on the parasitic patches are in the opposite direction, thus the predominant current flows in  $+x$  direction. When  $\omega t = 90^\circ$ , the surface current on longer parasitic patches flows in  $-y$  direction, while currents on the probe and shorter parasitic patches are in the opposite direction. Therefore, a dominant  $-y$  directed current flow is observed. It can be seen that the surface current distributions at  $\omega t = 270^\circ$  are equal in magnitude and opposite in phase to  $\omega t = 90^\circ$ . As the time changes, the surface current located at the azimuth angle turns in counter clockwise direction. Consequently, the polarization sense is right-hand circular polarization in  $+z$  direction.

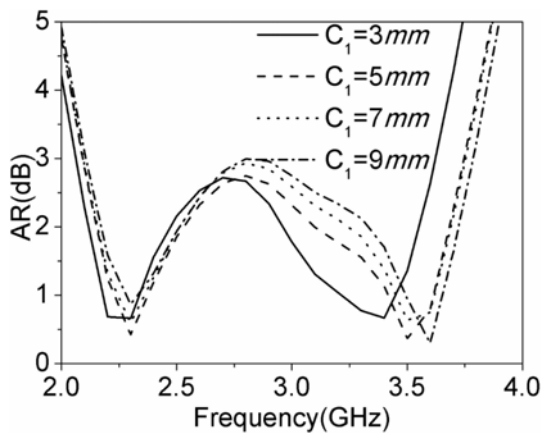


**Figure 3.** The AR of the proposed antenna with different  $C_1$ .

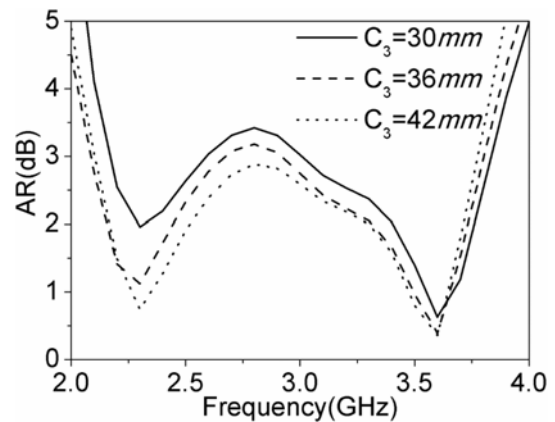


**Figure 4.** The AR of the proposed antenna with different  $C_3$ .

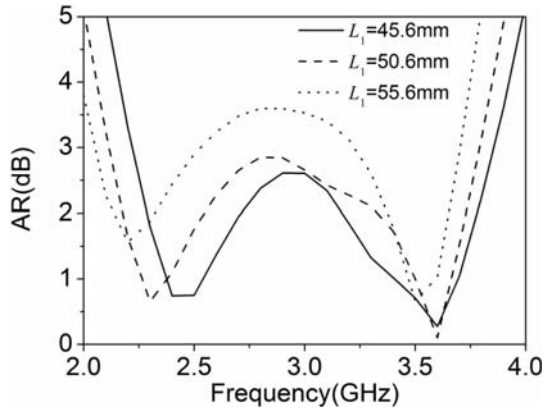


**Figure 5.** The AR of the proposed antenna with different  $L_1$ .

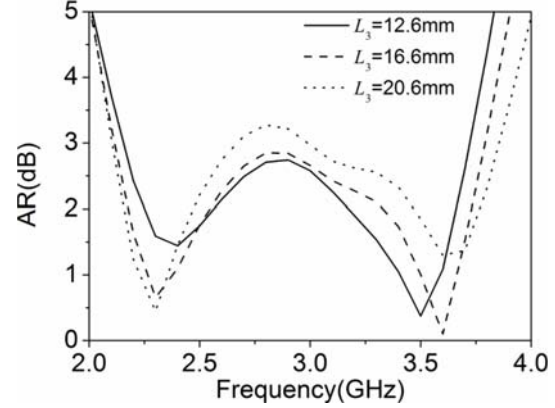


**Figure 6.** The AR of the proposed antenna with different  $L_3$ .

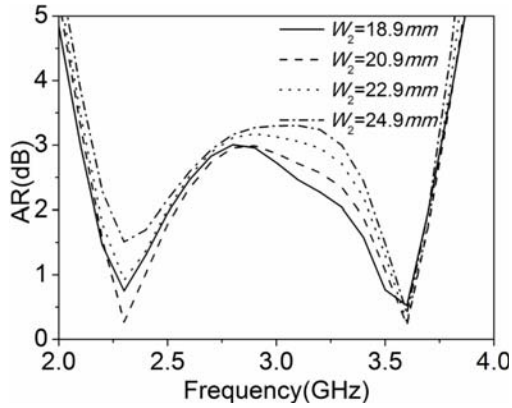


**Figure 7.** The AR of the proposed antenna with different  $W_2$ .

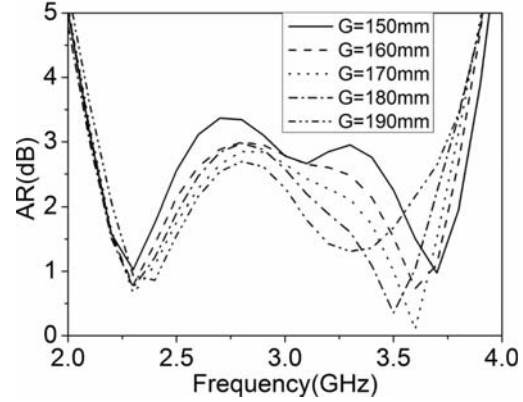


**Figure 8.** The AR of the proposed antenna with different  $G$ .

### 3. PARAMETER STUDY OF PROPOSED ANTENNA

The effects of different parameters are analyzed for further study. When one parameter is studied, the others are kept constant. The results present useful guidelines for practical design. As the variation of parameters have little effect on the impedance bandwidth, axial ratio bandwidth is taken seriously only.

Firstly, the slots etched on the longer parasitic patches are studied. The AR varies with rectangular slots width  $C_1$  is illustrated in Fig. 3. When  $C_1$  increases, the 3-dB axial ratio bandwidth of the proposed antenna is shifted toward the upper band. Fig. 4 shows the AR of the proposed antenna with different rectangular slots length  $C_3$ . It can be seen that, when  $C_3$  increases, the 3-dB axial ratio bandwidth is improved especially at lower band and changes little at upper band. These results suggest that the axial ratio bandwidth of the proposed antenna can be controlled by the rectangular slots. Therefore,  $C_1 = 9$  mm and  $C_3 = 42$  mm are selected for wide AR bandwidth.

Then the lengths of the parasitic elements,  $L_1$  and  $L_3$ , are analysed. The simulated results are shown in Fig. 5 and Fig. 6. When  $L_1$  increases, the AR bandwidth gets narrower at lower band. As  $L_3$  increases, the AR bandwidth gets larger, while the AR at 2.8 GHz will also get larger. For wide AR bandwidth operation,  $L_1$  and  $L_3$  are set to be 50.6 mm and 16.6 mm, respectively.

When the distance between L-shaped probe and parasitic patches increases, the energy conveyed from the probe to parasitic patches decreases, which may influence the AR bandwidth, thus the gap ( $W_2$ ) is analyzed. Fig. 7 shows the AR varies with  $W_2$ . It can be seen that the 3-dB axial ratio bandwidth goes into narrower when the distance  $W_2$  increases. For wideband operation,  $W_2$  is set to be 18.9 mm.

Also the effect of the dimension ( $G$ ) of the ground plane in AR is studied. The simulated results are shown in Fig. 8. It can be seen from the figure that the dimension ( $G$ ) has great effect on the AR bandwidth. With the increase of  $G$ , the AR becomes smaller around 3 GHz, but the AR bandwidth gets narrower in upper band. For wideband operation,  $G$  is set to be 170 mm.

#### 4. RESULTS AND DISCUSSION

To verify the analysis, the proposed antenna is produced and measured. Fig. 9 presents the simulated and measured VSWR and AR. The results show that the measured results agree well with the simulated. The impedance bandwidth for  $VSWR \leq 2$  is 81.25% from 1.9 GHz to 4.5 GHz. The reason for the little discrepancy may be the manufacturing process consisting of welding procedure and the manual fitting. The measured 3-dB axial ratio bandwidth is 56.2% from 2.11 GHz to 3.77 GHz, almost the same with the simulated one.

The measured normalized radiation patterns in the  $xoz$ -plane and  $yo z$ -plane are shown in Fig. 10. The polarization sense is right-hand circular polarization (RHCP) while the cross polarization is left-hand circular polarization (LHCP), which agrees well with the analysis before. The radiation pattern at 2.4 GHz is unidirectional and symmetric with the backward radiation efficiently suppressed. But at upper band, the beamwidth becomes wider and the cross-polarization gets larger. Fig. 11 illustrates the measured and simulated antenna gain. The measured antenna gain varies from 5 dBic to 9.2 dBic over working band, which is a little lower than the simulated one. The difference between measured and simulated results may be attributed to the measured environment effect and the tolerances in the manufacturing process.

A comparison between the proposed antenna and those single-feed antennas reported earlier is described in Table 2, which indicates that the proposed antenna delivers a much wider 3-dB axial ratio bandwidth. The average antenna gain of proposed antenna is larger than most antennas except [4].

**Table 2.** Performance of the proposed antenna and other single-feed circularly polarized antenna.

Ref. No.	VSWR $\leq 2$ Bandwidth	3-dB axial ratio bandwidth	Average antenna gain
[3]	63.9%	10%	5.7 dBic
[4]		13.5%	8.6 dBic
[5]	22.5%	19.4%	5.5 dBic
[6]	50.2%	27%	6.2 dBic
[7]	73.3%	47.7%	6.8 dBic
proposed	82.4%	56.2%	7.7 dBic

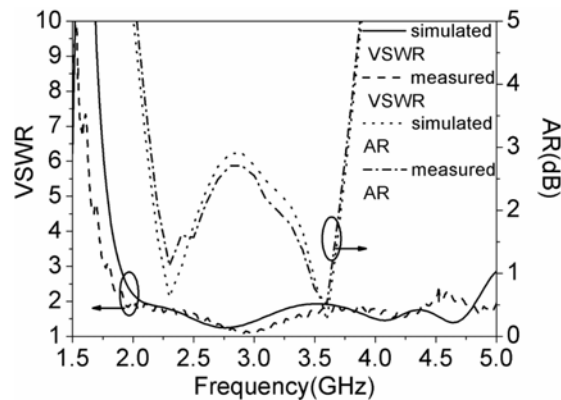


**Figure 9.** Simulated and measured VSWRs and ARs of the proposed antenna.

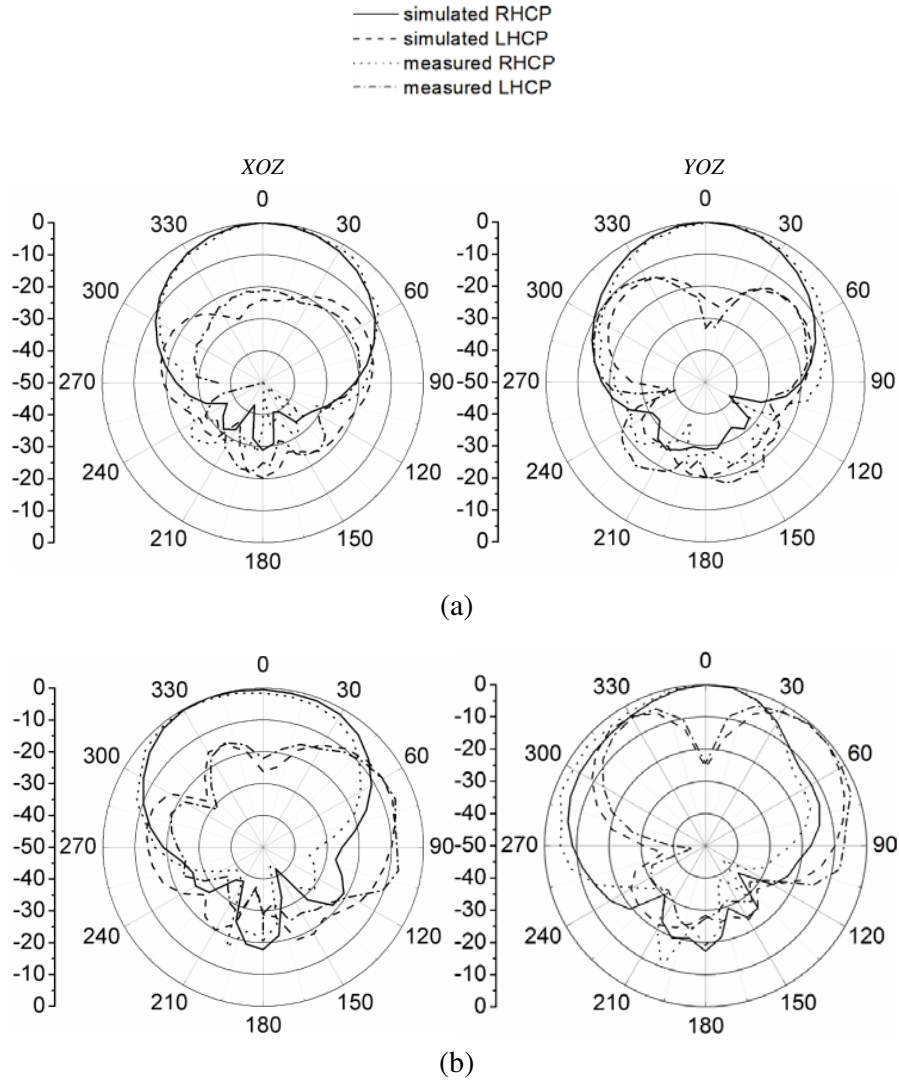


**Figure 10.** Simulated and measured normalized radiation pattern. (a) 2.4 GHz, (b) 3.5 GHz.

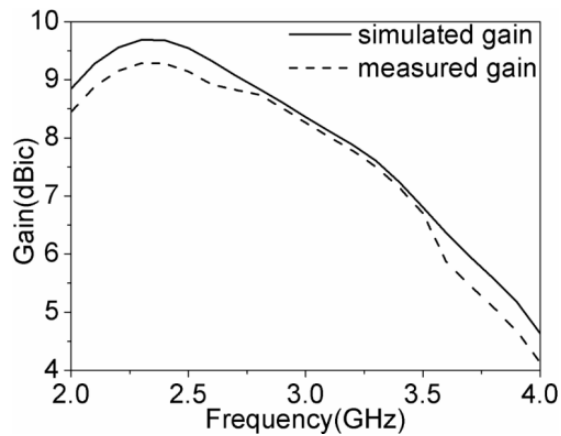


**Figure 11.** Simulated and measured antenna gains.

## 5. CONCLUSION

A novel single-feed wideband circularly polarized patch antenna with four parasitic patches is investigated. To improve the 3-dB axial ratio bandwidth, rectangular slots are etched on the longer parasitic patches and L-shaped slots etched on the shorter parasitic patches, respectively. By the modification of the structure, the proposed patch antenna delivers an impedance bandwidth of 82.4% from 2 GHz to 4.8 GHz and a wide 3-dB axial ratio of 56.2% from 2.11 GHz to 3.77 GHz. The measured results agree well with the simulated ones.

## ACKNOWLEDGMENT

This work was supported in part by the National Natural Science Foundation of China (Grant No. 61201022), and in part by the Fundamental Research Funds for the Central Universities (Grant No. JB150224).

## REFERENCES

1. Bian, L., Y.-X. Guo, L. C. Ong, and X.-Q. Shi, "Wideband circularly-polarized patch antenna," *IEEE Trans. Antennas Propag.*, Vol. 54, 2682–2686, 2006.
2. Hu, Y.-J., W.-P. Ding, W.-M. Ni, and W.-Q. Cao, "Broadband circularly polarized cavity-backed slot antenna array with four linearly polarized disks located in a single circular slot," *IEEE Antennas Wireless Propog. Lett.*, Vol. 11, 496–499, 2012.
3. Guo, Y.-X. and D. C. H. Tan, "Wideband single-feed circularly polarized patch antenna with conical radiation pattern," *IEEE Antennas Wireless Propog. Lett.*, Vol. 8, 924–926, 2009.
4. Wang, Z., S. Fang, S. Fu, and S. Jia, "Single-fed broadband circularly polarized stacked patch antenna with horizontally meandered strip for universal UHF RFID applications," *Microw. Opt. Technol. Lett.*, Vol. 59, 1066–1073, 2011.
5. Chung, K. L., "A wideband circularly polarized H-shaped patch antenna," *IEEE Trans. Antennas Propag.*, Vol. 58, 3379–3383, 2010.
6. He, Y., W. He, and H. Wong, "A wideband circularly polarized cross-dipole antenna," *IEEE Antennas Wireless Propog. Lett.*, Vol. 13, 67–70, 2014.
7. Li, M. and K.-M. Luk, "A wideband circularly polarized antenna for microwave and millimeter-wave applications," *IEEE Trans. Antennas Propag.*, Vol. 62, 1872–1879, 2014.